Journal of Photochemistry & Photobiology, B: Biology 187 (2018) 136–140

Contents lists available at ScienceDirect

Journal of Photochemistry & Photobiology, B: Biology

journal homepage: www.elsevier.com/locate/jphotobiol

Confocal Raman microscopy reveals changes in chemical composition of wood surfaces exposed to artificial weathering

Toru Kanbayashi[a,*], Yutaka Kataoka[a], Atsuko Ishikawa[a], Masahiro Matsunaga[a], Masahiko Kobayashi[a], Makoto Kiguchi[b]

[a] Forest Research and Management Organization, Forestry and Forest Products Research Institute, Matsunosato 1, Ibaraki 305-8687, Japan
[b] College of Bioresource Sciences, Nihon University, Kameino 1866, Fujisawa, Kanagawa 252-0880, Japan

ARTICLE INFO

Keywords:
Wood
Weathering
Photodegradation
Confocal Raman microscopy
Cell wall

ABSTRACT

Weathering leads to rapid depolymerization and modification of wood chemical components. The present study aims to assess the structural and distributional changes in the main wood polymers, such as lignin and polysaccharides, located in the surface layers during weathering exposure. A confocal Raman microscopic technique, which is useful for evaluating the structure of molecules with a high spatial resolution, was utilized to examine the effects of weathering on the chemical composition of wood surfaces at the cellular level. Raman spectra showed that lignin degradation during weathering proceeds with the formation of *o*- and *p*-quinones, carbonyl groups, and certain types of C=C double bonds such as stilbene derivatives. Comparing the weathering conditions between light only and light plus water exposure, it was found that weathering in the presence of water significantly enhances the degradation of lignin. The Raman images exhibited that the degree of lignin degradation by light only exposure is according to the depth. However, in the case of light plus water exposure, lignin degradation in the outermost cell walls proceeded from both the exposed surface side and the lumen side of the cell walls. This study is expected to potentially promote development of more effective and efficient methods to protect wood surfaces against weathering.

1. Introduction

Wood has been recognized as an easily available and versatile material, and it has been subjected to deterioration by a variety of natural agents. In outdoor and above-ground applications, the severe environmental conditions lead to rapid depolymerization and modification of wood chemical components, followed by discoloration and surface roughening [1–4]. These changes are due to the combination of several weathering factors, such as solar radiation, moisture, temperature, and atmospheric gases. Among these factors, solar radiation is suggested to exert the most damaging effect on wood cell walls. Ultraviolet (UV) rays in the sunlight produce free radical, and radical-induced oxidation significantly depolymerizes wood constituents [1,3,4]. Norrström estimated that 80%–95% of the degradation of wood by light exposure is attributed to the photodegradation of lignin [5]. Photodegradation results in the formation of new lignin chromophores, which cause discoloration, consisting mainly of quinone-type structures [6]. On the other hand, the depolymerized fragments are run-off by rain water causing surface roughening [1,3,4].

Weathering degradation of wood is a surface phenomenon. Using electron spin resonance, Hon and Ifju demonstrated that UV and visible light penetrate wood to a layer of 75 and 200 μm thickness, respectively [7]. Kataoka et al. suggested, on the basis of Fourier transform infrared (FTIR) microscopy measurements, that the depth of light penetration into the wood and the spreading rate of the degraded layer depend on the wavelength of light source and wood density [8–11]. In addition, considerable knowledge regarding the extent of weathering effect on woods has been accumulated by several research groups using various techniques, including histochemical staining [12,13], diffuse reflectance infrared Fourier transform spectroscopy [14,15], FTIR photoacoustic spectroscopy [16], and tensile strength measurement [17]. However, very little is known about the cellular-level chemical changes in wood surfaces during weathering.

Raman spectroscopy is a powerful tool for analyzing the molecular structures of organic and inorganic compounds [18]. Conventional Raman spectroscopy and other special techniques including Fourier transform Raman and resonance Raman spectroscopies, have been used to study light-induced photoyellowing of pulps [19–22] and weathered wood [23–26] and bamboo [27]. Recently, confocal Raman microscopy, combining a Raman spectrometer with an optical microscope,

* Corresponding author.
E-mail address: kanbayashi@ffpri.affrc.go.jp (T. Kanbayashi).

https://doi.org/10.1016/j.jphotobiol.2018.08.016
Received 12 June 2018; Received in revised form 8 August 2018; Accepted 13 August 2018
Available online 16 August 2018
1011-1344/

has been applied to topochemical analyses of wood cell walls with a high spatial resolution and without any pretreatment [28–35]. In our previous study, we successfully conducted depth profiling analysis of photodegraded wood surfaces using confocal Raman microscopy [36].

This study aimed to reveal the structural and distributional changes in the main wood polymers (lignin and polysaccharides) located in the surface layers during weathering exposure. The micro-scale local investigations were performed by confocal Raman microscopy.

2. Materials and Methods

2.1. Wood Samples

Wood samples were obtained from the sapwood of air-dried Japanese cedar (*Cryptomeria japonica* D. Don). These samples were cut into blocks at dimensions of 140 (longitudinal) × 25 (radial) × 9 (tangential) mm^3. The radial surface of each block was smoothed with a planer machine before exposure to artificial weathering.

2.2. Artificial Weathering Conditions

The radial face of wood blocks was exposed to artificial weathering in a weather-o-meter (Ci4000, Atlas, USA) for up to 500 h with a black panel temperature of 65 °C and chamber temperature of 38 °C. The weathering regime involved continuous exposure to xenon arc light source (0.51 W/m^2 at 340 nm) and 18 min of deionized water spraying every 2 h. A weathering series without water spray exposure has also been conducted. After a specified exposure period, 15 μm-thick cross sections with exposed surfaces (shown in Fig. 1) were prepared on a sliding microtome (TU-213, Yamato Kohki Industrial Co., Ltd., Japan) with dipping in water. Then, the thin sections were kept between glass slides and coverslips with a drop of water.

2.3. Confocal Raman Microscopy Measurements

The thin sections were analyzed by a confocal microRaman system (LabRAM ARAMIS, Horiba Jobin Yvon, France) equipped with a confocal microscope (BX41, Olympus, Japan), a 100× air objective (MPLN, NA = 0.9, Olympus), and a 532 nm diode-pumped solid-state laser (Ventus VIS 532, Laser Quantum, UK). The theoretical (diffraction limited) lateral resolution on the sample approximated 0.36 μm (0.61λ/NA), where λ is the wavelength of the laser and NA is the numerical aperture of the microscope objective. The incident laser power on the sample approximated 13 mW. No damage caused by the laser irradiation was observed. Raman scattered light was detected by a charge-coupled device camera placed behind either a 300- or 1800-lines/mm grating. The confocal aperture diameter was 300 μm in all experiments. The Raman spectra were recorded in the point analysis in 10 cycles, with each cycle consisting of a 1 s integration time for one spot. Ten spectra were obtained and averaged, and the averaged spectra from 10 different locations were again averaged (Fig. S1). The 1800-lines/mm grating was used in the point analysis. For Raman imaging, measurements were conducted every 0.7 μm step, and the spectra were obtained by averaging 4 cycles, each with a 0.1 s integration time. The 300-lines/mm grating was used for imaging. All the measurement positions were located on latewood.

The LabSpec5 software (Horiba Jobin Yvon) was used for spectral and image processing and analysis. To remove the background from the fluorescence, the raw spectral data were baseline-corrected. The smoothing was performed with the Savizky–Golay algorithm to reduce the spectral noise. In the point analysis, the Raman spectra were normalized by the intensity of the band at 1096 cm^{-1}, which is due to C – O and C – C stretching in polysaccharides [37]. In focus, the spectra ranged from 850 cm^{-1} to 3150 cm^{-1}. However, no spectral features were identified in the region from 1800 cm^{-1} to 2700 cm^{-1} before nor after weathering. Therefore, this region is not presented. The Raman bands from cellulose and hemicellulose are referred to as polysaccharides as they cannot be distinguished in the Raman spectra of wood [38,39].

3. Results and Discussion

3.1. Raman Spectral Analysis

Fig. 2 shows the averaged Raman spectra obtained from the outermost tracheids (described in Fig. 1) exposed to light only. Although most of the polysaccharides-related band intensities showed no significant changes, the lignin-related band intensities decreased to a more significant or lesser degree (Fig. 2A). The lignin bands at 1139, 1193, 1270, and 1330 cm^{-1}, which are assigned to coniferyl aldehyde, phenol, C – O of aryl – OH and aryl – O – CH_3, and aliphatic O – H bending, respectively [40], rapidly decreased in intensity with prolonged exposure time. On the other hand, the intensity of the prominent 1596 cm^{-1} band due to aromatic ring stretching [40] showed a relatively gentle reduction. These changes indicate that the structure of lignin polymer was partially degraded, whereas most of the aromatic rings remained after 500 h of light-only exposure.

The band region from 1510 cm^{-1} to 1770 cm^{-1}, which predominantly resulted from lignin features, showed several marked changes (Fig. 2B). The band at 1655 cm^{-1}, arising from the ethylenic C=C bond in coniferyl alcohol and the γ – C = O bond in coniferyl aldehyde [40], decreased, whereas several new peaks increased gradually with increased exposure time. The appearances of the bands at 1555 and 1673 cm^{-1} represent the formation of *o*- and *p*-quinone type structures [21,41], respectively. These structures are the key chromophores causing wood discoloration. The weak unassigned peaks at 1530, 1540, 1667, and 1700 cm^{-1} may be attributable to several lignin oxidation products. Increases were also observed in the intensities of the band at 1629 cm^{-1} and the broad band around 1740 cm^{-1}, which are due to the C=C bond of stilbene [41,42] and carbonyl groups [43], respectively. The aromatic band at 1596 cm^{-1} broadened and shifted toward a high-frequency range upon prolonged exposure. The band broadening and shifting in this spectral region imply progressive changes, such as the formation of C=O and C=C structures, in the substitution pattern in lignin.

Fig. 3 shows the averaged Raman spectra acquired from the

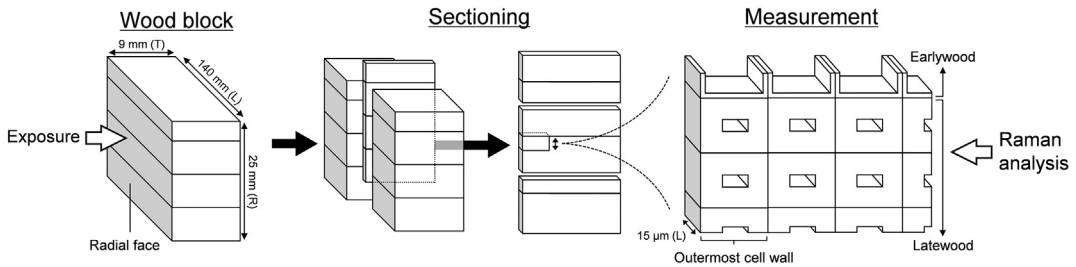

Fig. 1. Procedure for preparation of thin cross-sections along the weathered sample and the enlarged view of measurement area for Raman analyses. *L*, longitudinal; *R*, radial; *T*, tangential.